BABAR-PUB-08/022
SLAC-PUB-13322

Direct CP, Lepton Flavor and Isospin Asymmetries in the Decays $B \to K^{(*)}\ell^+\ell^-$

B. Aubert,[1] M. Bona,[1] Y. Karyotakis,[1] J. P. Lees,[1] V. Poireau,[1] E. Prencipe,[1] X. Prudent,[1] V. Tisserand,[1] J. Garra Tico,[2] E. Grauges,[2] L. Lopez[ab],[3] A. Palano[ab],[3] M. Pappagallo[ab],[3] G. Eigen,[4] B. Stugu,[4] L. Sun,[4] G. S. Abrams,[5] M. Battaglia,[5] D. N. Brown,[5] R. N. Cahn,[5] R. G. Jacobsen,[5] L. T. Kerth,[5] Yu. G. Kolomensky,[5] G. Lynch,[5] I. L. Osipenkov,[5] M. T. Ronan,[5,*] K. Tackmann,[5] T. Tanabe,[5] C. M. Hawkes,[6] N. Soni,[6] A. T. Watson,[6] H. Koch,[7] T. Schroeder,[7] D. Walker,[8] D. J. Asgeirsson,[9] B. G. Fulsom,[9] C. Hearty,[9] T. S. Mattison,[9] J. A. McKenna,[9] M. Barrett,[10] A. Khan,[10] V. E. Blinov,[11] A. D. Bukin,[11] A. R. Buzykaev,[11] V. P. Druzhinin,[11] V. B. Golubev,[11] A. P. Onuchin,[11] S. I. Serednyakov,[11] Yu. I. Skovpen,[11] E. P. Solodov,[11] K. Yu. Todyshev,[11] M. Bondioli,[12] S. Curry,[12] I. Eschrich,[12] D. Kirkby,[12] A. J. Lankford,[12] P. Lund,[12] M. Mandelkern,[12] E. C. Martin,[12] D. P. Stoker,[12] S. Abachi,[13] C. Buchanan,[13] J. W. Gary,[14] F. Liu,[14] O. Long,[14] B. C. Shen,[14,*] G. M. Vitug,[14] Z. Yasin,[14] L. Zhang,[14] V. Sharma,[15] C. Campagnari,[16] T. M. Hong,[16] D. Kovalskyi,[16] M. A. Mazur,[16] J. D. Richman,[16] T. W. Beck,[17] A. M. Eisner,[17] C. J. Flacco,[17] C. A. Heusch,[17] J. Kroseberg,[17] W. S. Lockman,[17] T. Schalk,[17] B. A. Schumm,[17] A. Seiden,[17] L. Wang,[17] M. G. Wilson,[17] L. O. Winstrom,[17] C. H. Cheng,[18] D. A. Doll,[18] B. Echenard,[18] F. Fang,[18] D. G. Hitlin,[18] I. Narsky,[18] T. Piatenko,[18] F. C. Porter,[18] R. Andreassen,[19] G. Mancinelli,[19] B. T. Meadows,[19] K. Mishra,[19] M. D. Sokoloff,[19] P. C. Bloom,[20] W. T. Ford,[20] A. Gaz,[20] J. F. Hirschauer,[20] M. Nagel,[20] U. Nauenberg,[20] J. G. Smith,[20] K. A. Ulmer,[20] S. R. Wagner,[20] R. Ayad,[21,†] A. Soffer,[21,‡] W. H. Toki,[21] R. J. Wilson,[21] D. D. Altenburg,[22] E. Feltresi,[22] A. Hauke,[22] H. Jasper,[22] M. Karbach,[22] J. Merkel,[22] A. Petzold,[22] B. Spaan,[22] K. Wacker,[22] M. J. Kobel,[23] W. F. Mader,[23] R. Nogowski,[23] K. R. Schubert,[23] R. Schwierz,[23] J. E. Sundermann,[23] A. Volk,[23] D. Bernard,[24] G. R. Bonneaud,[24] E. Latour,[24] Ch. Thiebaux,[24] M. Verderi,[24] P. J. Clark,[25] W. Gradl,[25] S. Playfer,[25] J. E. Watson,[25] M. Andreotti[ab],[26] D. Bettoni[a],[26] C. Bozzi[a],[26] R. Calabrese[ab],[26] A. Cecchi[ab],[26] G. Cibinetto[ab],[26] P. Franchini[ab],[26] E. Luppi[ab],[26] M. Negrini[ab],[26] A. Petrella[ab],[26] L. Piemontese[a],[26] V. Santoro[ab],[26] R. Baldini-Ferroli,[27] A. Calcaterra,[27] R. de Sangro,[27] G. Finocchiaro,[27] S. Pacetti,[27] P. Patteri,[27] I. M. Peruzzi,[27,§] M. Piccolo,[27] M. Rama,[27] A. Zallo,[27] A. Buzzo[a],[28] R. Contri[ab],[28] M. Lo Vetere[ab],[28] M. M. Macri[a],[28] M. R. Monge[ab],[28] S. Passaggio[a],[28] C. Patrignani[ab],[28] E. Robutti[a],[28] A. Santroni[ab],[28] S. Tosi[ab],[28] K. S. Chaisanguanthum,[29] M. Morii,[29] J. Marks,[30] S. Schenk,[30] U. Uwer,[30] V. Klose,[31] H. M. Lacker,[31] D. J. Bard,[32] P. D. Dauncey,[32] J. A. Nash,[32] W. Panduro Vazquez,[32] M. Tibbetts,[32] P. K. Behera,[33] X. Chai,[33] M. J. Charles,[33] U. Mallik,[33] J. Cochran,[34] H. B. Crawley,[34] L. Dong,[34] W. T. Meyer,[34] S. Prell,[34] E. I. Rosenberg,[34] A. E. Rubin,[34] Y. Y. Gao,[35] A. V. Gritsan,[35] Z. J. Guo,[35] C. K. Lae,[35] A. G. Denig,[36] M. Fritsch,[36] G. Schott,[36] N. Arnaud,[37] J. Béquilleux,[37] A. D'Orazio,[37] M. Davier,[37] J. Firmino da Costa,[37] G. Grosdidier,[37] A. Höcker,[37] V. Lepeltier,[37] F. Le Diberder,[37] A. M. Lutz,[37] S. Pruvot,[37] P. Roudeau,[37] M. H. Schune,[37] J. Serrano,[37] V. Sordini,[37,¶] A. Stocchi,[37] G. Wormser,[37] D. J. Lange,[38] D. M. Wright,[38] I. Bingham,[39] J. P. Burke,[39] C. A. Chavez,[39] J. R. Fry,[39] E. Gabathuler,[39] R. Gamet,[39] D. E. Hutchcroft,[39] D. J. Payne,[39] C. Touramanis,[39] A. J. Bevan,[40] C. K. Clarke,[40] K. A. George,[40] F. Di Lodovico,[40] R. Sacco,[40] M. Sigamani,[40] G. Cowan,[41] H. U. Flaecher,[41] D. A. Hopkins,[41] S. Paramesvaran,[41] F. Salvatore,[41] A. C. Wren,[41] D. N. Brown,[42] C. L. Davis,[42] K. E. Alwyn,[43] D. Bailey,[43] R. J. Barlow,[43] Y. M. Chia,[43] C. L. Edgar,[43] G. Jackson,[43] G. D. Lafferty,[43] T. J. West,[43] J. I. Yi,[43] J. Anderson,[44] C. Chen,[44] A. Jawahery,[44] D. A. Roberts,[44] G. Simi,[44] J. M. Tuggle,[44] C. Dallapiccola,[45] X. Li,[45] E. Salvati,[45] S. Saremi,[45] R. Cowan,[46] D. Dujmic,[46] P. H. Fisher,[46] K. Koeneke,[46] G. Sciolla,[46] M. Spitznagel,[46] F. Taylor,[46] R. K. Yamamoto,[46] M. Zhao,[46] P. M. Patel,[47] S. H. Robertson,[47] A. Lazzaro[ab],[48] V. Lombardo[a],[48] F. Palombo[ab],[48] J. M. Bauer,[49] L. Cremaldi,[49] V. Eschenburg,[49] R. Godang,[49,**] R. Kroeger,[49] D. A. Sanders,[49] D. J. Summers,[49] H. W. Zhao,[49] M. Simard,[50] P. Taras,[50] F. B. Viaud,[50] H. Nicholson,[51] G. De Nardo[ab],[52] L. Lista[a],[52] D. Monorchio[ab],[52] G. Onorato[ab],[52] C. Sciacca[ab],[52] G. Raven,[53] H. L. Snoek,[53] C. P. Jessop,[54] K. J. Knoepfel,[54] J. M. LoSecco,[54] W. F. Wang,[54] G. Benelli,[55] L. A. Corwin,[55] K. Honscheid,[55] H. Kagan,[55] R. Kass,[55] J. P. Morris,[55] A. M. Rahimi,[55] J. J. Regensburger,[55] S. J. Sekula,[55] Q. K. Wong,[55] N. L. Blount,[56] J. Brau,[56] R. Frey,[56] O. Igonkina,[56] J. A. Kolb,[56] M. Lu,[56] R. Rahmat,[56] N. B. Sinev,[56] D. Strom,[56] J. Strube,[56] E. Torrence,[56] G. Castelli[ab],[57] N. Gagliardi[ab],[57] M. Margoni[ab],[57] M. Morandin[a],[57] M. Posocco[a],[57] M. Rotondo[a],[57] F. Simonetto[ab],[57] R. Stroili[ab],[57] C. Voci[ab],[57] P. del Amo Sanchez,[58] E. Ben-Haim,[58] H. Briand,[58] G. Calderini,[58] J. Chauveau,[58] P. David,[58]

L. Del Buono,[58] O. Hamon,[58] Ph. Leruste,[58] J. Ocariz,[58] A. Perez,[58] J. Prendki,[58] S. Sitt,[58] L. Gladney,[59] M. Biasini[ab],[60] R. Covarelli[ab],[60] E. Manoni[ab],[60] C. Angelini[ab],[61] G. Batignani[ab],[61] S. Bettarini[ab],[61] M. Carpinelli[ab],[61, ††] A. Cervelli[ab],[61] F. Forti[ab],[61] M. A. Giorgi[ab],[61] A. Lusiani[ac],[61] G. Marchiori[ab],[61] M. Morganti[ab],[61] N. Neri[ab],[61] E. Paoloni[ab],[61] G. Rizzo[ab],[61] J. J. Walsh[a],[61] D. Lopes Pegna,[62] C. Lu,[62] J. Olsen,[62] A. J. S. Smith,[62] A. V. Telnov,[62] F. Anulli[a],[63] E. Baracchini[ab],[63] G. Cavoto[a],[63] D. del Re[ab],[63] E. Di Marco[ab],[63] R. Faccini[ab],[63] F. Ferrarotto[a],[63] F. Ferroni[ab],[63] M. Gaspero[ab],[63] P. D. Jackson[a],[63] L. Li Gioi[a],[63] M. A. Mazzoni[a],[63] S. Morganti[a],[63] G. Piredda[a],[63] F. Polci[ab],[63] F. Renga[ab],[63] C. Voena[a],[63] M. Ebert,[64] T. Hartmann,[64] H. Schröder,[64] R. Waldi,[64] T. Adye,[65] B. Franek,[65] E. O. Olaiya,[65] F. F. Wilson,[65] S. Emery,[66] M. Escalier,[66] L. Esteve,[66] S. F. Ganzhur,[66] G. Hamel de Monchenault,[66] W. Kozanecki,[66] G. Vasseur,[66] Ch. Yèche,[66] M. Zito,[66] X. R. Chen,[67] H. Liu,[67] W. Park,[67] M. V. Purohit,[67] R. M. White,[67] J. R. Wilson,[67] M. T. Allen,[68] D. Aston,[68] R. Bartoldus,[68] P. Bechtle,[68] J. F. Benitez,[68] R. Cenci,[68] J. P. Coleman,[68] M. R. Convery,[68] J. C. Dingfelder,[68] J. Dorfan,[68] G. P. Dubois-Felsmann,[68] W. Dunwoodie,[68] R. C. Field,[68] A. M. Gabareen,[68] S. J. Gowdy,[68] M. T. Graham,[68] P. Grenier,[68] C. Hast,[68] W. R. Innes,[68] J. Kaminski,[68] M. H. Kelsey,[68] H. Kim,[68] P. Kim,[68] M. L. Kocian,[68] D. W. G. S. Leith,[68] S. Li,[68] B. Lindquist,[68] S. Luitz,[68] V. Luth,[68] H. L. Lynch,[68] D. B. MacFarlane,[68] H. Marsiske,[68] R. Messner,[68] D. R. Muller,[68] H. Neal,[68] S. Nelson,[68] C. P. O'Grady,[68] I. Ofte,[68] A. Perazzo,[68] M. Perl,[68] B. N. Ratcliff,[68] A. Roodman,[68] A. A. Salnikov,[68] R. H. Schindler,[68] J. Schwiening,[68] A. Snyder,[68] D. Su,[68] M. K. Sullivan,[68] K. Suzuki,[68] S. K. Swain,[68] J. M. Thompson,[68] J. Va'vra,[68] A. P. Wagner,[68] M. Weaver,[68] C. A. West,[68] W. J. Wisniewski,[68] M. Wittgen,[68] D. H. Wright,[68] H. W. Wulsin,[68] A. K. Yarritu,[68] K. Yi,[68] C. C. Young,[68] V. Ziegler,[68] P. R. Burchat,[69] A. J. Edwards,[69] S. A. Majewski,[69] T. S. Miyashita,[69] B. A. Petersen,[69] L. Wilden,[69] S. Ahmed,[70] M. S. Alam,[70] J. A. Ernst,[70] B. Pan,[70] M. A. Saeed,[70] S. B. Zain,[70] S. M. Spanier,[71] B. J. Wogsland,[71] R. Eckmann,[72] J. L. Ritchie,[72] A. M. Ruland,[72] C. J. Schilling,[72] R. F. Schwitters,[72] B. W. Drummond,[73] J. M. Izen,[73] X. C. Lou,[73] F. Bianchi[ab],[74] D. Gamba[ab],[74] M. Pelliccioni[ab],[74] M. Bomben[ab],[75] L. Bosisio[ab],[75] C. Cartaro[ab],[75] G. Della Ricca[ab],[75] L. Lanceri[ab],[75] L. Vitale[ab],[75] V. Azzolini,[76] N. Lopez-March,[76] F. Martinez-Vidal,[76] D. A. Milanes,[76] A. Oyanguren,[76] J. Albert,[77] Sw. Banerjee,[77] B. Bhuyan,[77] H. H. F. Choi,[77] K. Hamano,[77] R. Kowalewski,[77] M. J. Lewczuk,[77] I. M. Nugent,[77] J. M. Roney,[77] R. J. Sobie,[77] T. J. Gershon,[78] P. F. Harrison,[78] J. Ilic,[78] T. E. Latham,[78] G. B. Mohanty,[78] H. R. Band,[79] X. Chen,[79] S. Dasu,[79] K. T. Flood,[79] Y. Pan,[79] M. Pierini,[79] R. Prepost,[79] C. O. Vuosalo,[79] and S. L. Wu[79]

(The *BABAR* Collaboration)

[1] *Laboratoire de Physique des Particules, IN2P3/CNRS et Université de Savoie, F-74941 Annecy-Le-Vieux, France*
[2] *Universitat de Barcelona, Facultat de Fisica, Departament ECM, E-08028 Barcelona, Spain*
[3] *INFN Sezione di Bari[a]; Dipartmento di Fisica, Università di Bari[b], I-70126 Bari, Italy*
[4] *University of Bergen, Institute of Physics, N-5007 Bergen, Norway*
[5] *Lawrence Berkeley National Laboratory and University of California, Berkeley, California 94720, USA*
[6] *University of Birmingham, Birmingham, B15 2TT, United Kingdom*
[7] *Ruhr Universität Bochum, Institut für Experimentalphysik 1, D-44780 Bochum, Germany*
[8] *University of Bristol, Bristol BS8 1TL, United Kingdom*
[9] *University of British Columbia, Vancouver, British Columbia, Canada V6T 1Z1*
[10] *Brunel University, Uxbridge, Middlesex UB8 3PH, United Kingdom*
[11] *Budker Institute of Nuclear Physics, Novosibirsk 630090, Russia*
[12] *University of California at Irvine, Irvine, California 92697, USA*
[13] *University of California at Los Angeles, Los Angeles, California 90024, USA*
[14] *University of California at Riverside, Riverside, California 92521, USA*
[15] *University of California at San Diego, La Jolla, California 92093, USA*
[16] *University of California at Santa Barbara, Santa Barbara, California 93106, USA*
[17] *University of California at Santa Cruz, Institute for Particle Physics, Santa Cruz, California 95064, USA*
[18] *California Institute of Technology, Pasadena, California 91125, USA*
[19] *University of Cincinnati, Cincinnati, Ohio 45221, USA*
[20] *University of Colorado, Boulder, Colorado 80309, USA*
[21] *Colorado State University, Fort Collins, Colorado 80523, USA*
[22] *Technische Universität Dortmund, Fakultät Physik, D-44221 Dortmund, Germany*
[23] *Technische Universität Dresden, Institut für Kern- und Teilchenphysik, D-01062 Dresden, Germany*
[24] *Laboratoire Leprince-Ringuet, CNRS/IN2P3, Ecole Polytechnique, F-91128 Palaiseau, France*
[25] *University of Edinburgh, Edinburgh EH9 3JZ, United Kingdom*
[26] *INFN Sezione di Ferrara[a]; Dipartimento di Fisica, Università di Ferrara[b], I-44100 Ferrara, Italy*
[27] *INFN Laboratori Nazionali di Frascati, I-00044 Frascati, Italy*
[28] *INFN Sezione di Genova[a]; Dipartimento di Fisica, Università di Genova[b], I-16146 Genova, Italy*
[29] *Harvard University, Cambridge, Massachusetts 02138, USA*

[30]Universität Heidelberg, Physikalisches Institut, Philosophenweg 12, D-69120 Heidelberg, Germany
[31]Humboldt-Universität zu Berlin, Institut für Physik, Newtonstr. 15, D-12489 Berlin, Germany
[32]Imperial College London, London, SW7 2AZ, United Kingdom
[33]University of Iowa, Iowa City, Iowa 52242, USA
[34]Iowa State University, Ames, Iowa 50011-3160, USA
[35]Johns Hopkins University, Baltimore, Maryland 21218, USA
[36]Universität Karlsruhe, Institut für Experimentelle Kernphysik, D-76021 Karlsruhe, Germany
[37]Laboratoire de l'Accélérateur Linéaire, IN2P3/CNRS et Université Paris-Sud 11,
Centre Scientifique d'Orsay, B. P. 34, F-91898 Orsay Cedex, France
[38]Lawrence Livermore National Laboratory, Livermore, California 94550, USA
[39]University of Liverpool, Liverpool L69 7ZE, United Kingdom
[40]Queen Mary, University of London, London, E1 4NS, United Kingdom
[41]University of London, Royal Holloway and Bedford New College, Egham, Surrey TW20 0EX, United Kingdom
[42]University of Louisville, Louisville, Kentucky 40292, USA
[43]University of Manchester, Manchester M13 9PL, United Kingdom
[44]University of Maryland, College Park, Maryland 20742, USA
[45]University of Massachusetts, Amherst, Massachusetts 01003, USA
[46]Massachusetts Institute of Technology, Laboratory for Nuclear Science, Cambridge, Massachusetts 02139, USA
[47]McGill University, Montréal, Québec, Canada H3A 2T8
[48]INFN Sezione di Milano[a]; Dipartimento di Fisica, Università di Milano[b], I-20133 Milano, Italy
[49]University of Mississippi, University, Mississippi 38677, USA
[50]Université de Montréal, Physique des Particules, Montréal, Québec, Canada H3C 3J7
[51]Mount Holyoke College, South Hadley, Massachusetts 01075, USA
[52]INFN Sezione di Napoli[a]; Dipartimento di Scienze Fisiche,
Università di Napoli Federico II[b], I-80126 Napoli, Italy
[53]NIKHEF, National Institute for Nuclear Physics and High Energy Physics, NL-1009 DB Amsterdam, The Netherlands
[54]University of Notre Dame, Notre Dame, Indiana 46556, USA
[55]Ohio State University, Columbus, Ohio 43210, USA
[56]University of Oregon, Eugene, Oregon 97403, USA
[57]INFN Sezione di Padova[a]; Dipartimento di Fisica, Università di Padova[b], I-35131 Padova, Italy
[58]Laboratoire de Physique Nucléaire et de Hautes Energies,
IN2P3/CNRS, Université Pierre et Marie Curie-Paris6,
Université Denis Diderot-Paris7, F-75252 Paris, France
[59]University of Pennsylvania, Philadelphia, Pennsylvania 19104, USA
[60]INFN Sezione di Perugia[a]; Dipartimento di Fisica, Università di Perugia[b], I-06100 Perugia, Italy
[61]INFN Sezione di Pisa[a]; Dipartimento di Fisica,
Università di Pisa[b]; Scuola Normale Superiore di Pisa[c], I-56127 Pisa, Italy
[62]Princeton University, Princeton, New Jersey 08544, USA
[63]INFN Sezione di Roma[a]; Dipartimento di Fisica,
Università di Roma La Sapienza[b], I-00185 Roma, Italy
[64]Universität Rostock, D-18051 Rostock, Germany
[65]Rutherford Appleton Laboratory, Chilton, Didcot, Oxon, OX11 0QX, United Kingdom
[66]DSM/Irfu, CEA/Saclay, F-91191 Gif-sur-Yvette Cedex, France
[67]University of South Carolina, Columbia, South Carolina 29208, USA
[68]Stanford Linear Accelerator Center, Stanford, California 94309, USA
[69]Stanford University, Stanford, California 94305-4060, USA
[70]State University of New York, Albany, New York 12222, USA
[71]University of Tennessee, Knoxville, Tennessee 37996, USA
[72]University of Texas at Austin, Austin, Texas 78712, USA
[73]University of Texas at Dallas, Richardson, Texas 75083, USA
[74]INFN Sezione di Torino[a]; Dipartimento di Fisica Sperimentale, Università di Torino[b], I-10125 Torino, Italy
[75]INFN Sezione di Trieste[a]; Dipartimento di Fisica, Università di Trieste[b], I-34127 Trieste, Italy
[76]IFIC, Universitat de Valencia-CSIC, E-46071 Valencia, Spain
[77]University of Victoria, Victoria, British Columbia, Canada V8W 3P6
[78]Department of Physics, University of Warwick, Coventry CV4 7AL, United Kingdom
[79]University of Wisconsin, Madison, Wisconsin 53706, USA

We measure branching fractions and integrated rate asymmetries for the rare decays $B \to K^{(*)}\ell^+\ell^-$, where $\ell^+\ell^-$ is either e^+e^- or $\mu^+\mu^-$, using a sample of 384 million $B\overline{B}$ events collected with the *BABAR* detector at the PEP-II e^+e^- collider. We find no evidence for direct *CP* or lepton-flavor asymmetries. However, for dilepton masses below the J/ψ resonance, we find evidence for unexpectedly large isospin asymmetries in both $B \to K\ell^+\ell^-$ and $B \to K^*\ell^+\ell^-$ which differ respectively by 3.2σ and 2.7σ, including systematic uncertainties, from the Standard Model expectations.

PACS numbers: 13.20.He

The decays $B \to K^{(*)}\ell^+\ell^-$, where $\ell^+\ell^-$ is either e^+e^- or $\mu^+\mu^-$, arise from flavor-changing neutral current processes that are forbidden at tree level in the Standard Model (SM). The lowest-order SM processes contributing to these decays are a W^+W^- box diagram, and the radiative photon and electroweak Z penguin diagrams [1]. Their amplitudes are expressed in terms of hadronic form factors and effective Wilson coefficients C_7^{eff}, C_9^{eff} and C_{10}^{eff}, representing the electromagnetic penguin diagram, and the vector part and the axial-vector part of the Z penguin and W^+W^- box diagrams, respectively [2]. New physics contributions may enter the penguin and box diagrams at the same order as the SM diagrams, modifying the Wilson coefficients from their SM expectations [3].

We report results herein on exclusive branching fractions, direct *CP* asymmetries, the ratio of rates to di-muon and di-electron final states, and isospin asymmetries, measured in two regions of dilepton mass squared chosen to exclude the region of the J/ψ resonance: a low q^2 region $0.1 < q^2 \equiv m^2_{\ell\ell} < 7.02\,\mathrm{GeV}^2/c^4$ and a high q^2 region $q^2 > 10.24\,\mathrm{GeV}^2/c^4$. We also present results for the two regions combined. The $\psi(2S)$ resonance is removed from the high q^2 region by vetoing events with $12.96 < q^2 < 14.06\,\mathrm{GeV}^2/c^4$. For $K^*e^+e^-$ final states, we also report results in extended low and extended combined q^2 regions including events $q^2 < 0.1\,\mathrm{GeV}^2/c^4$, where there is an enhanced coupling to the photonic penguin amplitude unique to this mode. Recent *BABAR* results on angular observables using the same dataset and similar event selection as is used here are reported in [1].

The $B \to K\ell^+\ell^-$ branching fraction is predicted to be $(0.35 \pm 0.12) \times 10^{-6}$, while $B \to K^*\ell^+\ell^-$ for $q^2 > 0.1\,\mathrm{GeV}^2/c^4$ is expected to be roughly three times larger at $(1.19 \pm 0.39) \times 10^{-6}$ [3]. The $\sim 30\%$ uncertainties are due to lack of knowledge about the form factors that model the hadronic effects in the $B \to K$ and $B \to K^*$ transitions. Thus, measurements of decay rates to exclusive final states are less suited to searches for new physics than rate asymmetries, where many theory uncertainties cancel [4].

The direct *CP* asymmetry

$$A_{CP}^{K^{(*)}} \equiv \frac{\mathcal{B}(\overline{B} \to \overline{K}^{(*)}\ell^+\ell^-) - \mathcal{B}(B \to K^{(*)}\ell^+\ell^-)}{\mathcal{B}(\overline{B} \to \overline{K}^{(*)}\ell^+\ell^-) + \mathcal{B}(B \to K^{(*)}\ell^+\ell^-)} \quad (1)$$

is expected to be $O(10^{-3})$ in the SM, but new physics at the electroweak scale could produce a significant enhancement [5].

The ratio of rates to di-muon and di-electron final states

$$R_{K^{(*)}} \equiv \frac{\mathcal{B}(B \to K^{(*)}\mu^+\mu^-)}{\mathcal{B}(B \to K^{(*)}e^+e^-)} \quad (2)$$

is unity in the SM to within a few percent [6]. In two-Higgs-doublet models, including supersymmetry, these ratios are sensitive to the presence of a neutral Higgs boson, which might, at large $\tan\beta$, increase $R_{K^{(*)}}$ by $\sim 10\%$ [7]. In the region $q^2 < (2m_\mu)^2$, where only the e^+e^- modes are allowed, there is a large enhancement of $B \to K^*e^+e^-$ due to a $1/q^2$ scaling of the photon penguin. The expected SM value of R_{K^*} including this region is 0.75 [6], and we fit the K^* dataset over the extended combined and extended low q^2 regions in order to test this prediction.

The *CP*-averaged isospin asymmetry

$$A_I^{K^{(*)}} \equiv \frac{\mathcal{B}(B^0 \to K^{(*)0}\ell^+\ell^-) - r\mathcal{B}(B^\pm \to K^{(*)\pm}\ell^+\ell^-)}{\mathcal{B}(B^0 \to K^{(*)0}\ell^+\ell^-) + r\mathcal{B}(B^\pm \to K^{(*)\pm}\ell^+\ell^-)} \quad (3)$$

where $r = \tau_0/\tau_+ = 1/(1.07 \pm 0.01)$ is the ratio of the B^0 and B^+ lifetimes [8], has a SM expectation of $+6-13\%$ as $q^2 \to 0\,\mathrm{GeV}^2/c^4$ [9]. This is consistent with the measured asymmetry of $3\pm3\%$ in $B \to K^*\gamma$ [8]. A calculation of the predicted K^{*+} and K^{*0} rates integrated over the low q^2 region gives $A_I^{K^*} = -0.005 \pm 0.020$ [10, 11]. In the high q^2 region, contributions from charmonium states may provide an additional source of isospin asymmetry, although the measured asymmetry in $J/\psi\,K^{(*)}$ is at most a few percent [8].

We use a data sample of 384 million $B\overline{B}$ pairs collected at the $\Upsilon(4S)$ resonance with the *BABAR* detector [12] at the PEP-II asymmetric-energy e^+e^- collider at SLAC. Our selection of charged and neutral particle candidates, as well as reconstruction of π^0, K^0_S and K^* candidates, are described at [1]. We reconstruct signal events in ten separate final states containing an e^+e^- or $\mu^+\mu^-$ pair, and a $K^0_S(\to \pi^+\pi^-)$, K^+, or $K^*(892)$ candidate with an invariant mass $0.82 < M(K\pi) < 0.97\,\mathrm{GeV}/c^2$. We reconstruct K^{*0} candidates in the final state $K^+\pi^-$, and K^{*+} candidates in the final states $K^+\pi^0$ and $K^0_S\pi^+$ (charge conjugation is implied throughout except as explicitly noted). We also study final states $K^{(*)}h^\pm\mu^\mp$, where h is a track with no particle identification requirement applied, to characterize backgrounds from hadrons misidentified as muons.

$B \to K^{(*)}\ell^+\ell^-$ decays are reconstructed using the kinematic variables $m_{\rm ES} = \sqrt{s/4 - p_B^{*2}}$ and $\Delta E = E_B^* - \sqrt{s}/2$, where p_B^* and E_B^* are the B momentum and energy in the $\Upsilon(4S)$ center-of-mass (CM) frame, and $\sqrt{s}$ is the total CM energy. We define a fit region $m_{\rm ES} > 5.2\,\mathrm{GeV}/c^2$, with $-0.07 < \Delta E < 0.04$ ($-0.04 < \Delta E < 0.04$) GeV for e^+e^- ($\mu^+\mu^-$) final states in the low and extended low q^2 region, and $-0.08 < \Delta E < 0.05$ ($-0.05 < \Delta E < 0.05$) GeV for high q^2.

The main backgrounds arise from random combinations of leptons from semileptonic B and D decays, which are suppressed through the use of neural networks (NN)

whose construction is described in detail in [1]. For each of the ten final states we use separate NN optimized to suppress either continuum or $B\overline{B}$ backgrounds in the low, extended low or high q^2 regions. We use simulated samples of signal and background events in the construction of the NN, and assume rates consistent with accepted values [8].

There is a further background contribution from $B \to D(\to K^{(*)}\pi)\pi$ decays, where both pions are misidentified as leptons. The pion misidentification rates are 2-3% for muons and <0.1% for electrons, so this background is only significant in the $\mu^+\mu^-$ final states. We veto these events by assigning the pion mass to a muon candidate, and requiring the invariant mass of the hypothetical $K^{(*)}\pi$ system to be outside the range 1.84-1.90 GeV/c^2. After all the above selections have been applied, the final reconstruction efficiency for signal events varies from 3.5% for $K^+\pi^0\mu^+\mu^-$ for the combined q^2 region, to 22% for $K^+\pi^-e^+e^-$ in the high q^2 region.

We perform unbinned maximum likelihood fits to $m_{\rm ES}$ distributions to obtain signal and background yields. We use an ARGUS shape [13] to describe the combinatorial background, allowing the shape parameter to float in the fits. For the signal, we use a fixed Gaussian shape unique to each final state, with mean and width determined from fits to the analogous final states in the vetoed $J/\psi K^{(*)}$ events. We account for a small residual contribution from misidentified hadrons by constructing a probability density function (pdf) using $K^{(*)}h^\pm\mu^\mp$ events weighted by the probability for the $h^\pm$ to be misidentified as a muon. We also account for background events that peak in the $m_{\rm ES}$ signal region, arising from charmonium events that escape the veto, and for contributions from misreconstructed signal events. We test our fits in each final state using the large samples of vetoed $J/\psi K^{(*)}$ and $\psi(2S)K^{(*)}$ events, and find that all the branching fractions are in good agreement with accepted values [14]. We perform simultaneous fits for $A_{CP}^{K^{(*)}}$, $R_{K^{(*)}}$ and $A_I^{K^{(*)}}$ summed over all the signal modes that contribute to the particular measurement.

We estimate the statistical significance of our fits by generating ensembles of 1000 datasets for each of the ten final states in each q^2 region of interest, and fitting each dataset with the full fit model described above. These tests also confirm the unbiased nature and proper error scaling of our fit methodology.

For the total $B \to K\ell^+\ell^-$ and $B \to K^*\ell^+\ell^-$ branching fractions averaged assuming isospin and lepton-flavor symmetry, we measure $(0.394^{+0.073}_{-0.069} \pm 0.020) \times 10^{-6}$ and $(1.11^{+0.19}_{-0.18} \pm 0.07) \times 10^{-6}$, respectively, where the first uncertainty is statistical and the second is systematic. Complete branching fraction results in all final states and q^2 regions, along with the statistical significance of each measurement and frequentist upper limits for measurements with $< 4\sigma$ statistical significance, are available online [15]. All results are in good agreement with previous measurements [8].

Table I summarizes the results for $A_{CP}^{K^{(*)}}$. In the fits to the separate B and $\overline{B}$ datasets in charge-conjugate final states, we assume a common background ARGUS shape parameter. Our final results are consistent with the SM expectation of negligible direct CP asymmetry. Table II shows the results for R_K and R_{K^*}, which are also consistent with the SM expectations.

Table III shows the results for the isospin asymmetry $A_I^{K^{(*)}}$. We directly fit the data for $A_I^{K^{(*)}}$ taking into account the differing lifetimes of B^0 and B^+. Figure 1 shows the charged and neutral low q^2 datasets with overlaid fit projections. We find no significant isospin asymmetries in the high and combined q^2 regions, or for $K^*e^+e^-$ fits in the extended regions. However, we find evidence for large negative asymmetries in the low q^2 region.

We calculate the statistical significance with which a null isospin asymmetry hypothesis is rejected using the change in log likelihood $\sqrt{2\Delta \ln \mathcal{L}}$ between the nominal fit to the data and a fit with $A_I^{K^{(*)}} = 0$ fixed. Figure 2 shows the likelihood curves obtained from the $K\ell^+\ell^-$ and $K^*\ell^+\ell^-$ fits. The parabolic nature of the curves in the $A_I^{K^{(*)}} > -1$ region demonstrates the essentially Gaussian nature of our fit results in the physical region, and the right-side axis of Figure 2 shows purely statistical significances based on Gaussian coverage. Incorporating the relatively small systematic uncertainties as a scaling factor on the change in log likelihood, the significance in the low q^2 region that $A_I^{K^{(*)}}$ is different from zero is 3.2σ for $K\ell^+\ell^-$ and 2.7σ for $K^*\ell^+\ell^-$. We have verified these confidence intervals by performing fits to ensembles of

TABLE I: $A_{CP}^{K^{(*)}}$ results in each relevant q^2 region. The uncertainties are statistical and systematic, respectively.

Mode	combined q^2	low q^2	high q^2
$K^+\ell^+\ell^-$	$-0.18^{+0.18}_{-0.18} \pm 0.01$	$-0.18^{+0.19}_{-0.19} \pm 0.01$	$-0.09^{+0.36}_{-0.39} \pm 0.02$
$K^{*0}\ell^+\ell^-$	$0.02^{+0.20}_{-0.20} \pm 0.02$	$-0.23^{+0.38}_{-0.38} \pm 0.02$	$0.17^{+0.24}_{-0.24} \pm 0.02$
$K^{*+}\ell^+\ell^-$	$0.01^{+0.26}_{-0.24} \pm 0.02$	$0.10^{+0.25}_{-0.24} \pm 0.02$	$-0.18^{+0.45}_{-0.55} \pm 0.04$
$K^*\ell^+\ell^-$	$0.01^{+0.16}_{-0.15} \pm 0.01$	$0.01^{+0.21}_{-0.20} \pm 0.01$	$0.09^{+0.21}_{-0.21} \pm 0.02$

TABLE II: $R_{K^{(*)}}$ results in each q^2 region. The extended ("ext.") regions are relevant only for R_{K^*}. The uncertainties are statistical and systematic, respectively.

q^2 Region	R_{K^*}	R_K
combined	$1.37^{+0.53}_{-0.40} \pm 0.09$	$0.96^{+0.44}_{-0.34} \pm 0.05$
ext. combined	$1.10^{+0.42}_{-0.32} \pm 0.07$	—
low	$1.01^{+0.58}_{-0.44} \pm 0.08$	$0.40^{+0.30}_{-0.23} \pm 0.02$
ext. low	$0.56^{+0.29}_{-0.23} \pm 0.04$	—
high	$2.15^{+1.42}_{-0.78} \pm 0.15$	$1.06^{+0.81}_{-0.51} \pm 0.06$

TABLE III: $A_I^{K^{(*)}}$ results in each q^2 region. The uncertainties are statistical and systematic, respectively. The last table row shows $K^*e^+e^-$ results for the extended regions.

Mode	combined q^2	low q^2	high q^2
$K\mu^+\mu^-$	$0.13^{+0.29}_{-0.37}\pm0.04$	$-0.91^{+1.2}_{-\infty}\pm0.18$	$0.39^{+0.35}_{-0.46}\pm0.04$
Ke^+e^-	$-0.73^{+0.39}_{-0.50}\pm0.04$	$-1.41^{+0.49}_{-0.69}\pm0.04$	$0.21^{+0.32}_{-0.41}\pm0.03$
$K\ell^+\ell^-$	$-0.37^{+0.27}_{-0.34}\pm0.04$	$-1.43^{+0.56}_{-0.85}\pm0.05$	$0.28^{+0.24}_{-0.30}\pm0.03$
$K^*\mu^+\mu^-$	$-0.00^{+0.36}_{-0.26}\pm0.05$	$-0.26^{+0.50}_{-0.34}\pm0.05$	$-0.08^{+0.37}_{-0.27}\pm0.05$
$K^*e^+e^-$	$-0.20^{+0.22}_{-0.20}\pm0.03$	$-0.66^{+0.19}_{-0.17}\pm0.02$	$0.32^{+0.75}_{-0.45}\pm0.03$
$K^*\ell^+\ell^-$	$-0.12^{+0.18}_{-0.16}\pm0.04$	$-0.56^{+0.17}_{-0.15}\pm0.03$	$0.18^{+0.36}_{-0.28}\pm0.04$
$K^*e^+e^-$	$-0.27^{+0.21}_{-0.18}\pm0.03$	$-0.25^{+0.20}_{-0.18}\pm0.03$	—

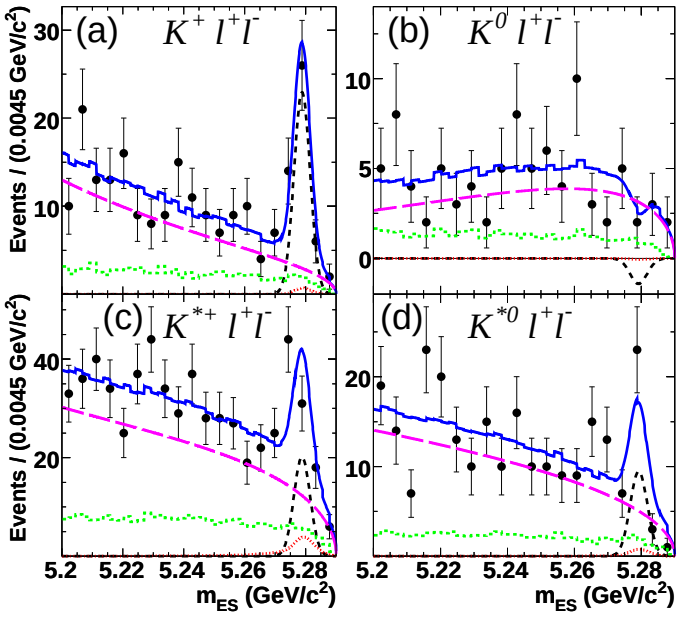

FIG. 1: Charged and neutral fit projections in the low q^2 region. Total fit [solid], combinatoric background [long dash], signal [medium dash], hadronic background [short dash], peaking background [dots].

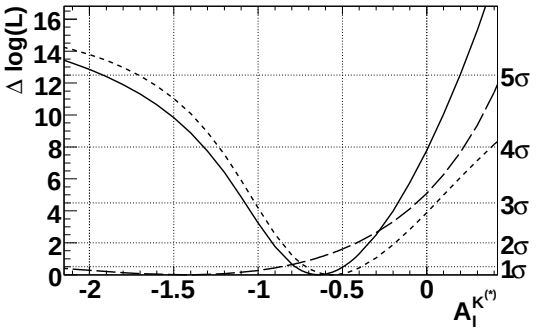

FIG. 2: Low q^2 region $A_I^{K^{(*)}}$ fit likelihood curves. $K\ell^+\ell^-$ [long dash], $K^*\ell^+\ell^-$ [short dash], $(K,K^*)\ell^+\ell^-$ [solid].

simulated datasets generated with $A_I^{K^{(*)}}=0$ fixed, and we find frequentist coverage consistent with the $\Delta\ln\mathcal{L}$ calculations. The highly negative $A_I^{K^{(*)}}$ values for both $K\ell^+\ell^-$ and $K^*\ell^+\ell^-$ at low q^2 suggest that this asymmetry may be insensitive to the hadronic final state, and so we sum the likelihood curves as shown in Figure 2 and obtain $A_I^{K^{(*)}}=-0.64^{+0.15}_{-0.14}\pm0.03$. Including systematics, this is a 3.9σ difference from a null $A_I^{K^{(*)}}$ hypothesis.

We consider systematic uncertainties associated with reconstruction efficiencies; hadronic background parameterization in di-muon final states; peaking background contributions obtained from simulated events; and possible *CP*, lepton flavor and isospin asymmetries in the background pdfs. We quantify the efficiency systematics using the vetoed $J/\psi K^{(*)}$ samples. These include charged track, π^0, and K^0_S reconstruction, particle identification, NN selection, and the ΔE and K^* mass selections. The largest contributions to the systematic uncertainties on the rates are particle identification, the characterization of the hadronic background and the signal $m_{\rm ES}$ pdf shape. All of these cancel at least partially in the rate asymmetries, and the final systematic uncertainties are small compared to the statistical ones.

We perform several additional checks of effects that might cause a bias in our final results. We vary the parameterization of the hadronic background pdfs, and of the random combinatorial background ARGUS shapes in the low q^2 region, to test the robustness of the large $A_I^{K^{(*)}}$ asymmetries. We remove all the NN selections, and perform separate fits to the two K^{*+} final states, and observe no significant variation in the $A_I^{K^{(*)}}$ results. To understand if an isospin asymmetry might be induced by the combinatorial background, we compare data and simulated background events within a larger region $|\Delta E|<0.25\,\text{GeV}$ outside our ΔE selection window and in the $5.2<m_{\rm ES}<5.27\,\text{GeV}/c^2$ region. We find that the numbers of simulated and data events in this larger region agree well. No signal isospin asymmetry is found using simulated events within the fit region.

In summary, we have measured branching fractions, and studied direct *CP* violation, ratios of rates to di-muon and di-electron final states, and isospin asymmetries in the rare decays $B\to K^{(*)}\ell^+\ell^-$. Our branching fraction results agree with both SM predictions and previous measurements. Our results for the direct *CP* asymmetries and lepton-flavor rate ratios are in good agreement with their respective SM predictions of zero and one. The isospin asymmetries in the high and combined q^2 regions are consistent with zero, but in the low q^2 region in both $B\to K\ell^+\ell^-$ and $B\to K^*\ell^+\ell^-$ we measure large negative asymmetries that are each about 3σ different from zero, including systematic uncertainties. Combining these results, we obtain $A_I^{K^{(*)}}=-0.64^{+0.15}_{-0.14}\pm0.03$, with a 3.9σ difference (including sys-

tematics) from $A_I^{K^{(*)}} = 0$. Such large negative asymmetries are unexpected in the SM, which predicts essentially no isospin asymmetry integrated over our low q^2 region and, as $q^2 \to 0$, an asymmetry of $\sim +10\%$, opposite in sign to our observation in the low q^2 region.

We are grateful for the excellent luminosity and machine conditions provided by our PEP-II colleagues, and for the substantial dedicated effort from the computing organizations that support *BABAR*. The collaborating institutions wish to thank SLAC for its support and kind hospitality. This work is supported by DOE and NSF (USA), NSERC (Canada), CEA and CNRS-IN2P3 (France), BMBF and DFG (Germany), INFN (Italy), FOM (The Netherlands), NFR (Norway), MES (Russia), MEC (Spain), and STFC (United Kingdom). Individuals have received support from the Marie Curie EIF (European Union) and the A. P. Sloan Foundation.

* Deceased
† Now at Temple University, Philadelphia, Pennsylvania 19122, USA
‡ Now at Tel Aviv University, Tel Aviv, 69978, Israel
§ Also with Università di Perugia, Dipartimento di Fisica, Perugia, Italy
¶ Also with Università di Roma La Sapienza, I-00185 Roma, Italy
** Now at University of South Alabama, Mobile, Alabama 36688, USA
†† Also with Università di Sassari, Sassari, Italy

[1] B. Aubert *et al.* [*BABAR* Collaboration], arXiv:0804.4412 (2008), submitted to PRD-RC.
[2] G. Buchalla, A. J. Buras and M. E. Lautenbacher, Rev. Mod. Phys. **68**, 1125 (1996).
[3] A. Ali, E. Lunghi, C. Greub and G. Hiller, Phys. Rev. D **66**, 034002 (2002).
[4] F. Kruger, L. M. Sehgal, N. Sinha and R. Sinha, Phys. Rev. D **61**, 114028 (2000) [Erratum-ibid. D **63**, 019901 (2001)].
[5] C. Bobeth, G. Hiller and G. Piranishvili, arXiv:0805.2525 (2008).
[6] G. Hiller and F. Kruger, Phys. Rev. D **69**, 074020 (2004).
[7] Q. S. Yan, C. S. Huang, W. Liao and S. H. Zhu, Phys. Rev. D **62**, 094023 (2000).
[8] Heavy Flavor Averaging Group, E. Barberio *et al.*, arXiv:0704.3575 (2007).
[9] T. Feldmann and J. Matias, JHEP **0301**, 074 (2003).
[10] M. Beneke, T. Feldmann and D. Seidel Eur. Phys. J. **C41**, 173 (2005).
[11] T. Feldmann, 5th Workshop on the CKM Unitary Triangle, Rome (2008).
[12] B. Aubert *et al.* [*BABAR* Collaboration], Nucl. Instrum. Meth. A **479**, 1 (2002).
[13] H. Albrecht *et al.* [ARGUS Collaboration], Z. Phys. C **48**, 543 (1990).
[14] W. M. Yao *et al.* [Particle Data Group], J. Phys. G **33** (2006) 1.
[15] See EPAPS Document No. E-PRLTAO-102-060910 for branching fraction results to accompany this article. For more information on EPAPS, see http://www.aip.org/pubservs/epaps.html.

Table I shows the total and partial branching fractions in $B \to K^{(*)}\ell^+\ell^-$ modes, along with statistical and systematic errors, and the statistical significance of each measurement. To calculate significance, the data are refit with a null signal hypothesis and the change in $\ln \mathcal{L}$ with the nominal fit is used to determine the significance. For measurements with a statistical significance less than 4.0σ, we fit ensembles of toy datasets derived from our observations in the data to compute frequentist upper limits at the 90% confidence level, in which only fit results which give a physical signal yield are used. The combined q^2 results are scaled to account for the regions of the total dilepton mass distribution which are vetoed and not included in the fits.

TABLE I: Branching fractions by mode and q^2 region with statistical and systematic errors, respectively. The statistical significance of each measurement is given parenthetically. 90% confidence level upper limits are provided for measurements with $< 4\sigma$ statistical significance.

Mode	combined q^2 (10^{-6})	90% UL	low q^2 (10^{-6})	90% UL	high q^2 (10^{-6})	90% UL
$K^0\mu^+\mu^-$	$0.49^{+0.29}_{-0.25}$ ±0.03 (2.2σ)	0.99	$0.01^{+0.15}_{-0.13}$ ±0.01 (0.0σ)	0.31	$0.25^{+0.16}_{-0.14}$ ±0.02 (1.9σ)	0.53
$K^+\mu^+\mu^-$	$0.41^{+0.16}_{-0.15}$ ±0.02 (3.0σ)	0.62	$0.123^{+0.082}_{-0.071}$ ±0.007 (1.8σ)	0.25	$0.116^{+0.079}_{-0.072}$ ±0.010 (1.7σ)	0.24
$K^0e^+e^-$	$0.08^{+0.15}_{-0.12}$ ±0.01 (0.6σ)	0.36	$-0.049^{+0.061}_{-0.049}$ ±0.004 (0.0σ)	0.10	$0.177^{+0.118}_{-0.091}$ ±0.011 (2.3σ)	0.38
$K^+e^+e^-$	$0.51^{+0.12}_{-0.11}$ ±0.02 (5.8σ)	–	$0.308^{+0.070}_{-0.062}$ ±0.013 (6.7σ)	–	$0.125^{+0.062}_{-0.055}$ ±0.006 (2.5σ)	0.21
$K^{*+}\mu^+\mu^-$	$1.46^{+0.79}_{-0.75}$ ±0.12 (2.0σ)	2.55	$0.75^{+0.49}_{-0.45}$ ±0.07 (1.7σ)	1.48	$0.78^{+0.43}_{-0.40}$ ±0.06 (2.1σ)	1.36
$K^{*0}\mu^+\mu^-$	$1.35^{+0.40}_{-0.37}$ ±0.10 (4.1σ)	–	$0.41^{+0.24}_{-0.21}$ ±0.04 (2.2σ)	0.83	$0.62^{+0.21}_{-0.19}$ ±0.05 (3.8σ)	0.97
$K^{*+}e^+e^-$	$1.38^{+0.47}_{-0.42}$ ±0.08 (3.7σ)	1.97	$1.06^{+0.31}_{-0.28}$ ±0.07 (4.7σ)	–	$0.19^{+0.23}_{-0.21}$ ±0.01 (0.9σ)	0.53
$K^{*0}e^+e^-$	$0.86^{+0.26}_{-0.24}$ ±0.05 (4.2σ)	–	$0.20^{+0.12}_{-0.11}$ ±0.01 (2.1σ)	0.42	$0.35^{+0.15}_{-0.13}$ ±0.02 (3.0σ)	0.60

In addition to the above results, we have also performed fits in extended q^2 regions for K^* di-electron final states, where a significant rate enhancement compared to that above $q^2 > 0.1\,\mathrm{GeV}^2/c^4$ is expected. Table II shows the total and partial branching fractions for these modes for extended q^2 regions.

TABLE II: Branching fractions for the extended q^2 regions with statistical and systematic errors, respectively.

Mode	combined q^2 (10^{-6})	low q^2 (10^{-6})
$B^+ \to K^{*+}e^+e^-$	$1.90^{+0.59}_{-0.55} \pm 0.11$	$1.32^{+0.41}_{-0.36} \pm 0.09$
$B^0 \to K^{*0}e^+e^-$	$1.02^{+0.30}_{-0.28} \pm 0.06$	$0.73^{+0.22}_{-0.19} \pm 0.04$

We also perform fits combining various hadronic and di-lepton final states which are then averaged assuming isospin and/or lepton-flavor symmetry. Table III shows branching fractions for the combined modes including statistical and systematic errors, statistical significance and upper limits for measurements with $< 4\sigma$ statistical significance.

TABLE III: Combined mode branching fractions by q^2 region with statistical and systematic errors, respectively. The statistical significance of each measurement is given parenthetically. 90% confidence level upper limits are provided for measurements with $< 4\sigma$ statistical significance.

Mode	combined q^2 (10^{-6})	90% UL	low q^2 (10^{-6})	90% UL	high q^2 (10^{-6})	90% UL
$K^0\ell^+\ell^-$	$0.21^{+0.15}_{-0.13}$ ±0.02 (1.7σ)	0.45	$-0.041^{+0.058}_{-0.047}$ ±0.004 (0.0σ)	0.09	$0.202^{+0.096}_{-0.081}$ ±0.013 (3.0σ)	0.36
$K^+\ell^+\ell^-$	$0.476^{+0.092}_{-0.086}$ ±0.022 (6.5σ)	–	$0.250^{+0.052}_{-0.047}$ ±0.010 (6.7σ)	–	$0.122^{+0.048}_{-0.044}$ ±0.006 (3.0σ)	0.19
$K\mu^+\mu^-$	$0.41^{+0.13}_{-0.12}$ ±0.02 (4.7σ)	–	$0.096^{+0.066}_{-0.059}$ ±0.006 (2.1σ)	0.21	$0.139^{+0.067}_{-0.062}$ ±0.008 (2.9σ)	0.25
Ke^+e^-	$0.388^{+0.090}_{-0.083}$ ±0.020 (5.6σ)	–	$0.217^{+0.051}_{-0.046}$ ±0.010 (5.9σ)	–	$0.132^{+0.050}_{-0.045}$ ±0.007 (3.5σ)	0.21
$K\ell^+\ell^-$	$0.394^{+0.073}_{-0.069}$ ±0.020 (7.3σ)	–	$0.181^{+0.039}_{-0.036}$ ±0.008 (6.1σ)	–	$0.135^{+0.040}_{-0.037}$ ±0.007 (4.5σ)	–
$K^{*0}\ell^+\ell^-$	$1.03^{+0.22}_{-0.21}$ ±0.07 (5.8σ)	–	$0.257^{+0.110}_{-0.098}$ ±0.02 (2.9σ)	0.44	$0.46^{+0.12}_{-0.11}$ ±0.03 (4.7σ)	–
$K^{*+}\ell^+\ell^-$	$1.40^{+0.40}_{-0.37}$ ±0.09 (4.2σ)	–	$0.98^{+0.26}_{-0.24}$ ±0.06 (4.9σ)	–	$0.34^{+0.21}_{-0.19}$ ±0.02 (1.8σ)	0.63
$K^*\mu^+\mu^-$	$1.35^{+0.35}_{-0.33}$ ±0.10 (5.3σ)	–	$0.47^{+0.21}_{-0.19}$ ±0.04 (3.2σ)	0.84	$0.65^{+0.18}_{-0.17}$ ±0.05 (4.7σ)	–
$K^*e^+e^-$	$0.99^{+0.23}_{-0.21}$ ±0.06 (5.6σ)	–	$0.42^{+0.13}_{-0.12}$ ±0.03 (4.3σ)	–	$0.30^{+0.12}_{-0.11}$ ±0.02 (3.1σ)	0.49
$K^*\ell^+\ell^-$	$1.11^{+0.19}_{-0.18}$ ±0.07 (7.7σ)	–	$0.43^{+0.11}_{-0.10}$ ±0.03 (5.3σ)	–	$0.42^{+0.10}_{-0.10}$ ±0.03 (5.3σ)	–